

Nanoscale

Accepted Manuscript



This is an *Accepted Manuscript*, which has been through the Royal Society of Chemistry peer review process and has been accepted for publication.

Accepted Manuscripts are published online shortly after acceptance, before technical editing, formatting and proof reading. Using this free service, authors can make their results available to the community, in citable form, before we publish the edited article. We will replace this *Accepted Manuscript* with the edited and formatted *Advance Article* as soon as it is available.

You can find more information about *Accepted Manuscripts* in the [Information for Authors](#).

Please note that technical editing may introduce minor changes to the text and/or graphics, which may alter content. The journal's standard [Terms & Conditions](#) and the [Ethical guidelines](#) still apply. In no event shall the Royal Society of Chemistry be held responsible for any errors or omissions in this *Accepted Manuscript* or any consequences arising from the use of any information it contains.

Simultaneously Tuning the Electric and Magnetic Plasmonic Response Using Capped Bi-metallic Nanoantennas[†]

Brian J. Roxworthy,^a and Kimani C. Toussaint, Jr.,^{*b}

We present a novel, capped bowtie nanoantenna capable of achieving simultaneous enhancement of electric and magnetic fields in a broad spectrum spanning visible to near-infrared frequencies. By controlling parameters including nanoantenna array spacing, cap thickness, and bowtie gap spacing, we show magnetic enhancements in excess of 3000 times the incident field, which are among the highest values reported to date. Further, electric field enhancements $> 10^4$ are obtained across the full parameter range. This is in contrast to diabolito antenna designs that achieve strong magnetic enhancement at the expense of mitigating the electrical resonance. We further show that this architecture achieves refractive index sensitivities of $\sim 700 \text{ nm} \cdot \text{RIU}^{-1}$. The combination of large, tunable electric and magnetic-field enhancements makes the capped-nanoantenna platform highly attractive for magnetic plasmonics, metamaterial engineering, nonlinear optics, and sensing applications.

1 Introduction

Plasmonic nanostructures are the subject of intense current research due to their ability to confine optical fields into deep sub-wavelength volumes, resulting in considerable electric field enhancement properties.¹ These properties have enabled breakthroughs in diverse applications including super-resolution imaging,^{2,3} single-molecule detection,⁴ surface enhanced Raman scattering (SERS),⁵ nanoscale heat generation,^{6,7} and optical manipulation.^{8,9} These advancements notwithstanding, there is an emerging interest in optical magnetism, i.e., generating optical frequency magnetic fields.^{10–12} Given that most materials exhibit a relative permeability of $\mu_r \sim 1$ above terahertz frequencies, plasmonic devices are required for engineering magnetic near-field enhancement in the optical regime.¹³ As such, the field of magnetic plasmonics has attracted much recent attention, due not only to interest in studying magnetic plasmons, but also for various potential applications such as low-loss plasmon propagation, magnetic sensors, metamaterial research, and nonlinear magnetics.^{11,14–16} To date, structures such as plasmonic oligomer molecules,¹¹ diabolito nanoantennas,¹² and metal-dielectric sandwiches,¹⁷ have been utilized to produce optical magnetism with enhancements up to 3000x the incident field.¹² The common approach is to engineer a large nanoscale current density in the structure in order to produce the largest possible magnetic field. However, a consequence of this is reduced charge density accumulation in nanoscale gap regions which mitigates the usually desirable electric field enhance-

ment.^{12,17}

In this paper, we demonstrate the simultaneous enhancement of both electric and magnetic fields using a novel platform based on an Au bowtie nanoantenna capped with a metallic Au or Ag slab. We show electric-field enhancements $> 10^4$ in the nanoscale gap and concurrent magnetic enhancements in excess of 3000x, which are among the highest reported to date.¹² In addition to a broad enhancement continuum spanning $\sim 600\text{--}2500 \text{ nm}$, these capped-bowtie nanoantenna arrays (c-BNAs) yield distinct resonances in the visible (VIS) and near-infrared (NIR), for both electric and magnetic fields. We show that, in general, using a bi-metallic structure consisting of an Ag cap and Au bowties results in a 10–15% larger enhancement compared to an all Au c-BNA structure. The NIR resonance can be easily tuned over a $\sim 500 \text{ nm}$ wavelength range by altering the cap thickness (t), whereas changing the bowtie gap size (g) enables a $\sim 50\text{-nm}$ wavelength tunability of the VIS resonance. Interestingly, we observe a simultaneous blue and red shift of the VIS and NIR resonances, respectively, as the gap size increases. The versatility of this platform to produce simultaneously large electric and magnetic-field enhancements over a broad spectral range makes c-BNAs highly attractive for applications in metamaterial engineering, SERS, and nonlinear optics.

2 Calculation Methods

A commercial FDTD solver (Lumerical Solutions) is used to calculate the electric and magnetic responses. The c-BNA structure is simulated by placing an Au or Ag cap of 85-nm width, 135-nm length, and varying thickness ($5 \leq t \leq 40\text{nm}$), symmetrically on top of a bowtie nanoantenna comprising two, tip-to-tip triangles of 120-nm height, 15-nm tip radius of curvature, 50-nm thickness and varying gap spacing ($10 \leq$

[†] Electronic Supplementary Information (ESI) available.

^a Department of Electrical and Computer Engineering, University of Illinois at Urbana-Champaign, Urbana, IL 61801, USA.

^b Department of Mechanical Science and Engineering, University of Illinois at Urbana-Champaign, Urbana, IL 61801, USA; E-mail: ktous-sai@illinois.edu

$g \leq 30$ nm). The nanoantenna structure is placed on an SiO₂ substrate and the local medium is air; refractive indices of the substrate and medium are 1.51 and 1, respectively, and the material parameters for Au and Ag are taken from Johnson and Christy.¹⁸ An infinite array with spacing $\Gamma = 400 - 600$ nm is simulated by using a rectangular region with periodic boundary conditions on the x and y boundaries; perfectly matched layers on the upper and lower z boundaries prevent spurious reflections by absorbing the field scattered from the structure. A refined mesh of $2 \times 2 \times 2$ nm encloses the structure in the center of the simulation region and ensures a high resolution of the confined electric and magnetic fields. The entire unit cell is illuminated with a plane wave spanning a spectral range of 350-4000 nm and the calculated field enhancements are the maximum values obtained in the gap region.

3 Results and Discussion

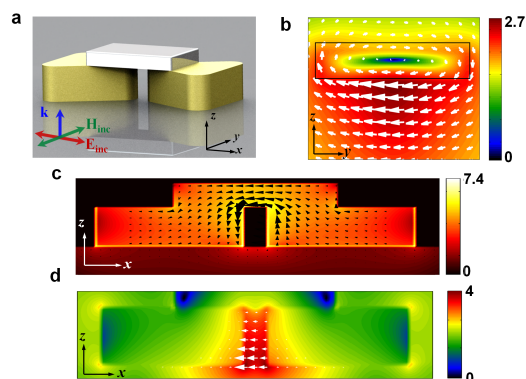


Fig. 1 Unit cell of the c-BNA structure comprising the nanoantenna and SiO₂ substrate; the wave vector and incident electric and magnetic-fields are represented by blue, red, and green arrows, respectively. Cross-sectional view of the (b) magnetic field produced in the gap by the (c) induced current density. The cross section of the metal cap is indicated by the black rectangle and white arrows represent the local magnetic field. (d) Cross-sectional of the electric field.

Figure 1 depicts the unit structure comprising the c-BNAs. The input electric field is polarized parallel to the long, tip-to-tip (x -) axis of the bowtie nanoantenna in order to generate a strong current density (\mathbf{J}) in the structure, which can be seen in Fig. 1(c). The magnetic field produced by \mathbf{J} is shown in the Fig. 1(b) and the local direction of the field is shown by white arrows; the local direction of the electric field is shown in Fig. 1(d). Typical electric and magnetic near-field distributions of the c-BNAs are plotted on a log scale and given in Fig. 2. Here, we observe the electric and magnetic-field enhancement, defined as $|\mathbf{E}/\mathbf{E}_0|^2$ and $|\mathbf{H}/\mathbf{H}_0|^2$, respectively, where \mathbf{E}

(\mathbf{H}) is the peak electric (magnetic) field and \mathbf{E}_0 (\mathbf{H}_0) is the input electric (magnetic) field amplitude. The field distributions in Figs. 2a and 2b correspond to the NIR and VIS resonances of the system, respectively. Evidently there are strong electric- and magnetic-field enhancements in the gap region for the c-BNAs in both the NIR and VIS resonances. Additionally, the fields are concentrated into a deep-subwavelength volume of $V_{VIS}/\lambda_{VIS}^3 \sim 10^{-4}$ and $V_{NIR}/\lambda_{NIR}^3 \sim 10^{-5}$ for the VIS and NIR resonances, respectively, where $V_{VIS} = V_{NIR}$ is the approximate mode volume and λ_{VIS} (λ_{NIR}) is the peak wavelength of the VIS (NIR) mode.¹⁹ The volume is taken to be the rectangular prism with side lengths of 20, 50, and 85 nm corresponding to the bowtie gap, bowtie height, and cap width, respectively.

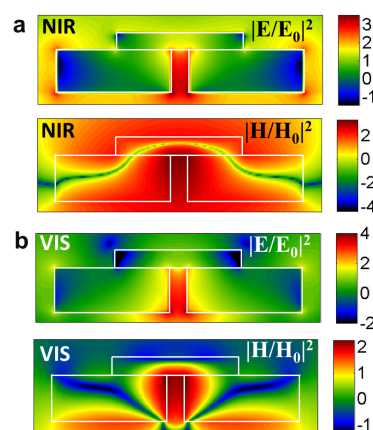


Fig. 2 Normalized electric and magnetic-intensities plotted on a log scale for the (a) NIR resonance and (b) VIS resonance of a structure with a $t = 20$ nm, $\Gamma = 425$ nm, and $g = 20$ nm.

The novel “dual enhancement” property, which is a unique feature of the c-BNA structure, can be attributed to simultaneous generation of a strong current density throughout the structure as well as charge density accumulation in the gap region of the bowtie. In particular, the magnetic-field enhancement originates from a current loop formed in the x - z plane that consists of the induced current density in the metal and a weaker displacement current in the SiO₂ substrate, evident in Fig. 1c, that closes the loop. Excitation of the c-BNA structure therefore produces a strong magnetic dipole moment orientated predominantly along the negative y -axis. In addition, significant charge accumulation occurs in the gap region of the bowties that is due to the lightning rod effect,^{1,20} which is responsible for the large electric-field enhancement of the c-BNAs.

In order to form a better understanding of the enhancement properties of the c-BNAs, we examine the spectral response as a function of cap thickness, t , for a bi-metallic structure consisting of Au bowties and an Ag cap with array spacing and

bowtie gap of $\Gamma = 425$ nm and $g = 20$ nm, respectively; results for the mono-metallic, Au c-BNAs and mono-metallic Ag c-BNAs can be found in the supplementary information.[†] Figure 3 shows that the spectra are dominated by two distinct resonance peaks located in the NIR and VIS, in addition to a broad enhancement continuum spanning from 600 to 2500nm, with a peak magnetic (electric) field enhancement $\sim 10^3$ ($> 10^4$). We see that increasing the cap thickness produces a blue shift for both resonances and reduces the NIR peak while increasing the VIS enhancement slightly. This leads to an overall shift of $\Delta\lambda_{NIR} \sim 500$ nm for the NIR peak, and thus demonstrates the wide spectral tunability of these nanoantennas.

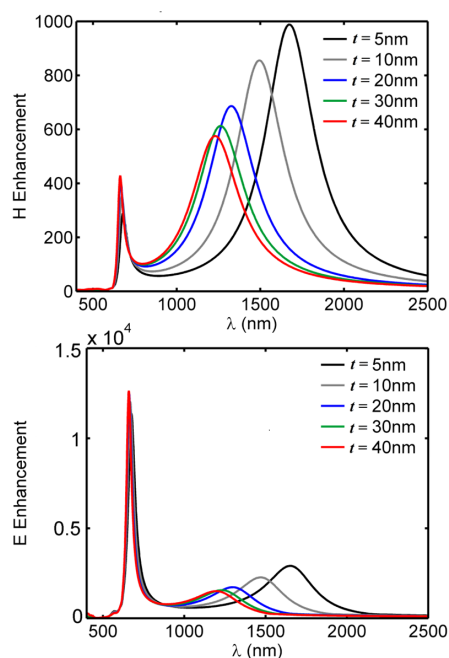


Fig. 3 Spectral response of the c-BNAs for the magnetic (left panel) and electric (right panel) fields as a function of varying cap thickness.

Comparing the results with the mono-metallic Au case, we find that the bi-metallic structure produces a 10-15% increase in the peak enhancement values with little change in the spectral locations of the resonances compared to mono-metallic Au c-BNAs. The extra enhancement can be attributed to the fact that losses associated with Ag are only 30% those of Au across the spectral window considered in this study.[†] For mono-metallic Ag c-BNAs, we find that both the electric and magnetic field enhancements are more than 50% larger compared to mono-metallic Au and bimetallic c-BNAs (with little change in the spectral location of the NIR and VIS peaks).[†] However, Ag nanostructures are rapidly oxidized upon environmental exposure, which degrades their plasmonic response and reduces their efficacy as sensors.²¹ Furthermore,

the Ag^+ ions present in oxidized Ag are toxic to biological species.²² Consequently, bi-metallic c-BNAs are better suited for sensing applications, compared to mono-Au c-BNAs, because they take advantage of increased field enhancement with reduced environmental degradation.

The blue shift introduced by varying cap thickness can be partially understood from a plasmon hybridization picture.^{1,23} Here, the charge density of the c-BNAs is represented by the superposition of elementary bowtie and cap charges: $\rho(\mathbf{r}) = \rho_{\text{cap}}(\mathbf{r}) + \rho_{\text{bowtie}}(\mathbf{r})$, where $\rho_{\text{cap}}(\mathbf{r})$ ($\rho_{\text{bowtie}}(\mathbf{r})$) is the charge density in the cap (bowtie) region; $\rho(\mathbf{r})$ is shown in Fig. 4. Note that the spatial charge density distribution in the mono-metallic case is indistinguishable from the bi-metallic case. Examination of the charge densities reveals that for the NIR resonance, the cap exhibits a quadrupole-like charge distribution with negative (positive) charge accumulation on the upper left (right) edges and positive (negative) charge accumulation on the lower left (right) edges. Additional charge signs are included in the cap region for clarity. Increasing t results in a larger charge separation between upper and lower edges, thereby reducing the Coulomb screening effect in $\rho_{\text{cap}}(\mathbf{r})$ and causing a blue shift in the plasmon resonance.²⁴ The full set of calculated $\rho(\mathbf{r})$ distributions is available in the supplementary information.[†] Similarly, we observe that as the length of the cap is increased along the x -axis, a blue shift occurs that can be attributed to increased separation of opposing charges on the cap,[†] which is consistent with the proposed hybridization model.

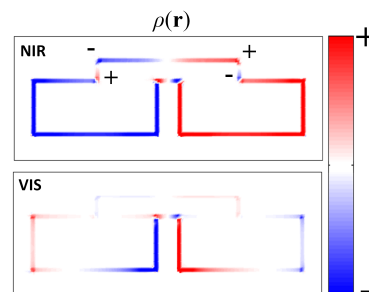


Fig. 4 Normalized charge density plots for the NIR (top panel) and VIS (bottom panel) modes in a bi-metallic c-BNA structure. The charge accumulation in the gap in the VIS case, due to the lightning rod effect, is not present in the NIR mode.

Given that $\rho_{\text{bowtie}}(\mathbf{r})$ does not change appreciably with cap thickness, the relative insensitivity of the VIS resonance to t suggests that this mode is dominated by the $\rho_{\text{bowtie}}(\mathbf{r})$ contribution. To verify this, we investigate the enhancement response as a function of bowtie gap spacing for both bi-metallic and mono-metallic structures. Figure 5 shows the magnetic and electric response of the c-BNAs as the gap separating the constituent triangles in the bowtie is increased from

10 to 30 nm. We note that the peak electric-field enhancement is a remarkable 2.5×10^4 in the gap, and that the peak magnetic-field enhancement $> 3 \times 10^3$. The VIS resonance experiences a blue shift of ~ 60 nm with increasing gap spacing that is accompanied by a reduction in the peak enhancement due to lower field confinement in larger gaps. This effect is observed in the hybridization model of longitudinally coupled plasmonic dimers^{23,24} and is consistent with the VIS resonance being governed primarily by $\rho_{\text{bowtie}}(\mathbf{r})$. Here, as g increases, the blue shift originates from reduced screening of the Coulombic restoring force acting on free electrons in the two triangles comprising the bowtie.^{23,25–27} Interestingly, the NIR resonance experiences an opposite-red shift with increasing g . Similar simultaneous red and blue shifts have been observed for split-ring resonator (SRR) geometries and occur due to coupling of induced magnetic and electric dipoles. This manifests as non-zero, off-diagonal terms in the polarizability tensor $\alpha = [\alpha_{EE} \alpha_{EH}; \alpha_{HE} \alpha_{HH}]$, where α_{EE} and α_{HH} represent the purely electric and magnetic polarizabilities of the structure, respectively, α_{HE} indicates the magnetic dipole induced by the incident electric field, and α_{EH} indicates an electric dipole induced by the incident magnetic field.²⁸ In the case of the c-BNAs, the redshift of the NIR mode with reduced coupling (increased g) indicates that this resonance is dominated by transversely coupled magnetic dipoles induced in neighboring nanoantennas.²⁶

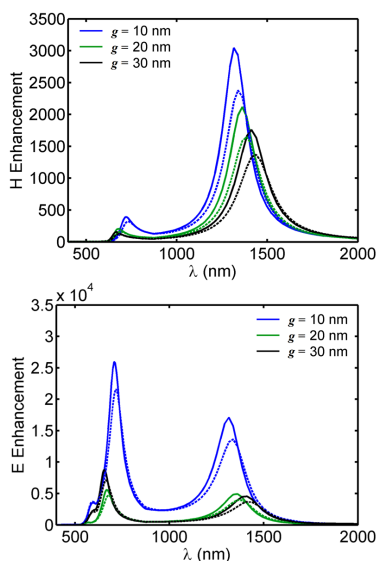


Fig. 5 Spectral responses of the c-BNAs as a function of the bowtie gap spacing. Solid (dotted) lines correspond to bi-metallic (mono-metallic) c-BNAs.

The dependence of the c-BNA magnetic response as a function of array spacing is given in Fig. 6. We see that as Γ decreases, both NIR and VIS modes experience a slight blue

shift. This result is consistent with related findings using SRR devices²⁶ and can be seen to arise due to the fact that the magnetic dipole moment is aligned perpendicular to the plane of the c-BNAs (the x - z plane), i.e. transverse coupling dominates in as Γ is increased. Moreover, increasing Γ leads to higher enhancement of the NIR mode, albeit at the expense of reduction of the VIS mode. Thus, Γ can be used as an additional parameter to selectively tune the c-BNA response. Despite the apparent similarities between the c-BNA and SRR systems, the former is unique with regards to the large field enhancements that are not present in SRRs. This marks an important distinction between the present work and previous efforts devoted towards SRRs, and thus warrants further investigation of capped nanoantenna systems.

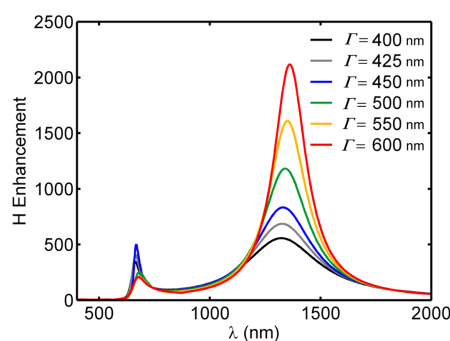


Fig. 6 Magnetic spectral response of bi-metallic c-BNAs as a function of array spacing.

The efficacy of the c-BNAs for sensing can be evaluated from the sensitivity δn to the local refractive index.²⁹ In order to estimate the sensitivity, we first calculate the shift in the VIS and NIR plasmon resonances from the respective peaks in the spectral absorption cross section, given by $\Delta\sigma$, as a function of the local index of refraction n . Figure 7 shows $\Delta\sigma$ for bi-metallic c-BNAs ($\Gamma = 425$ nm, $t = 20$ nm, $g = 20$ nm) for both the VIS and NIR modes, indicated by grey and red squares, respectively. As expected, a red shift is evident for both modes with increasing n and we see that the spectral location of both VIS and NIR resonances exhibits a linear dependence with n . It follows that the c-BNA sensitivity is given by the slope of the linear fit and has units of nm/refractive index unit (RIU); the VIS and NIR modes have sensitivities $\delta n_{VIS} = 270$ and $\delta n_{NIR} = 680$ nm·RIU⁻¹, respectively. Notably, δn_{NIR} is comparable to the particularly high values obtained from plasmonic mushroom array (1000 nm·RIU⁻¹)²⁹ and nanorice (800 nm·RIU⁻¹)³⁰ systems. For mono-metallic Au c-BNAs, δn_{NIR} (δn_{VIS}) is $\sim 20\%$ lower ($\sim 3\%$ higher) compared to the bi-metallic case.[†] The differences in δn between the two cases can be understood by examining their spectral absorption cross-sections ($\sigma_{abs}(\lambda)$).[†] For the NIR mode, mono-metallic c-BNAs have a significantly larger

value of σ_{abs} compared to the bi-metallic case, whereas for the VIS mode, the absorption of both structures is comparable. Thus, larger absorption associated with increased plasmon damping results in lower refractive index sensitivity for the c-BNAs.³¹ Overall, the high-sensitivity and exceptional field enhancement properties make c-BNAs an attractive architecture for chemical and biological sensing as well as studies in nonlinear optics and nonlinear magnetics.

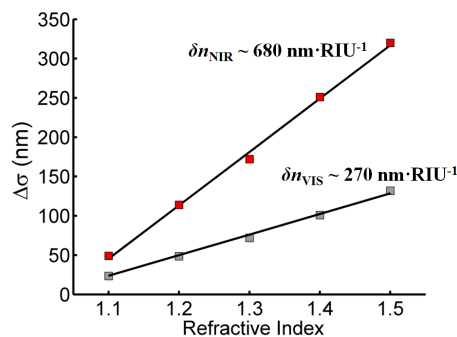


Fig. 7 Spectral sensitivity of the c-BNAs. Grey squares represent data for the VIS resonance whereas red squares indicate NIR results. Linear fits are included as black lines

4 Conclusion

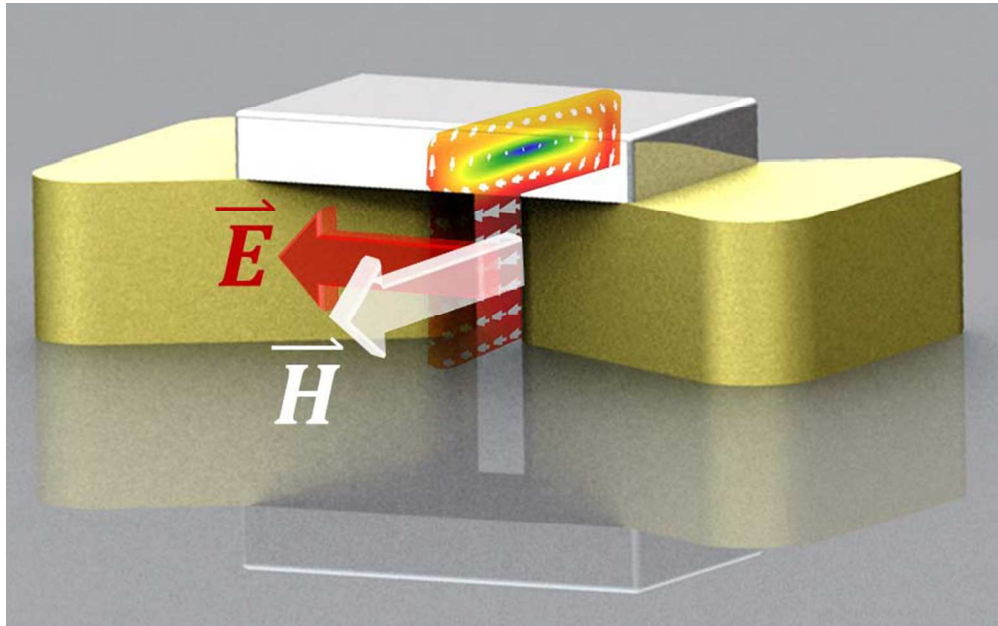
We have introduced a new class of capped plasmonic nanoantennas capable of simultaneous enhancement of magnetic and electric fields by more than 3 and 4 orders of magnitude at optical frequencies, respectively. Using the specific example of c-BNAs, we have shown that the magnetic plasmon response can be tuned across the VIS and NIR by simple adjustment of the cap thickness and bowtie gap spacing. Further, using Ag as the cap material, an additional $\sim 15\%$ increase in field enhancement can be achieved, which is attributed to decreased plasmon damping in Ag compared to Au. Using the plasmon hybridization model, we have identified that the NIR mode depends predominantly on the geometric properties of the cap whereas the VIS mode is dominated by contributions from the bowtie. Moreover, the resonance splitting effect, whereby increasing gap spacing introduces a blue (red) shift to the VIS (NIR) mode, is seen to originate from the coupling between electric and magnetic dipole modes in the system, in accordance with previous studies of split-ring resonators. The c-BNAs achieve a maximum refractive index sensitivity of $\sim 700 \text{ nm} \cdot \text{RIU}^{-1}$, making this platform attractive for high-sensitivity probing of chemical and biological systems. Overall, the exceptional field enhancement properties exhibited by the c-BNAs signify this architecture as an important advancement for not only magnetic plasmonics, but also for diverse applications in nonlinear optics, sensing, and nano-optics.

Acknowledgments

This work was partially supported by the National Science Foundation (NSF ECCS 10-25868).

References

- N. J. Halas, W.-S. Chang, S. Link and P. Nordlander, *Chem. Rev.*, 2011, **111**, 3913–3961.
- E. X. Jin and X. Xu, *Appl. Phys. Lett.*, 2005, **86**, 111106.
- K. A. Willets, *Phys. Chem. Chem. Phys.*, 2013, **15**, 5345–5354.
- P. Zijlstra, P. M. R. Paulo and M. Orrit, *Nature Nanotech.*, 2012, **7**, 379–382.
- S. Lal, S. Link and N. J. Halas, *Nature Photon.*, 2007, **1**, 641–648.
- G. Baffou and R. Quidant, *Laser Photon. Rev.*, 2013, **7**, 171–187.
- Z. J. Coppens, W. Li, D. G. Walker and J. G. Valentine, *Nano Lett.*, 2013, **13**, 1023–1028.
- B. J. Roxworthy, K. D. Ko, A. Kumar, K.-H. Fung, G. L. Liu, N. X. Fang and K. C. Toussaint, Jr., *Nano Lett.*, 2012, **12**, 796–801.
- B. J. Roxworthy and K. C. Toussaint, Jr., *Sci. Rep.*, 2012, **2**, 660.
- A. K. Sarychev, G. Shvets and V. M. Shalaev, *Phys. Rev. E*, 2006, **73**, 036609.
- N. Liu, S. Mukherjee, K. Bao, L. V. Brown, J. Dormuller, P. Nordlander and N. J. Halas, *Nano Lett.*, 2012, **12**, 364–369.
- T. Grosjean, M. Mivelle, F. I. Baida, G. W. Burr and U. C. Fischer, *Nano Lett.*, 2011, **11**, 1009–1013.
- A. N. Grigorenko, A. K. Geim, H. F. Gleeson, Y. Zhang, A. A. Firsov, I. Y. Khrushchev and J. Petrovich, *Nature*, 2005, **438**, 335–338.
- H. W. Kim, S. M. Koo, Q. H. Kim, K. Bao, J. E. Kihm, W. S. Bak, S. H. Eah, C. Lienau, H. Kim, P. Nordlander, N. J. Halas, N. K. Park and D.-S. Kim, *Nat. Commun.*, 2011, **2**, 451.
- C. M. Soukoulis, S. Linden and M. Wegener, *Science*, 2007, **315**, 47–49.
- M. W. Klein, C. Enkrich, M. Wegener and S. Linden, *Science*, 2006, **313**, 502–504.
- S. M. Wang, T. Li, H. Liu, F. M. Wang, S. N. Zhu and X. Zhang, *Opt. Express*, 2008, **16**, 3560–3565.
- P. B. Johnson and R. W. Christy, *Phys. Rev. B*, 1972, **6**, 4370–4379.
- S. A. Maier, *Opt. Express*, 2006, **14**, 1957–1964.
- J. H. Kang, D. S. Kim and Q. H. Park, *Phys. Rev. Lett.*, 2009, **102**, 093906.
- A. Henglein, *Chem. Mater.*, 1998, **10**, 444–450.
- C. N. Lok, C. M. Ho, R. Chen, Q. Y. He, W. Y. Yu, H. Sun, P. K. H. Tam, J. F. Chiu and C. M. Che, *J. Biol. Inorg. Chem.*, 2007, **12**, 527–534.
- E. Prodan, C. Radloff, N. J. Halas and P. Nordlander, *Science*, 2003, **302**, 419–422.
- P. K. Jain, W. Huang and M. El-Sayed, *Nano Lett.*, 2007, **7**, 2080–2088.
- P. K. Jain and M. El-Sayed, *Chem. Phys. Lett.*, 2010, **487**, 153–164.
- I. Sersic, M. Frimmer, E. Verhagen and A. F. Koenderink, *Phys. Rev. Lett.*, 2009, **103**, 213902.
- W. Rechberger, A. Hohenau, A. Leitner, J. R. Krenn, B. Lamprecht and F. R. Aussenegg, *Opt. Commun.*, 2003, **220**, 137–141.
- I. Sersic, C. Tuambilangana, T. Kampfrath and A. F. Koenderink, *Phys. Rev. B*, 2011, **83**, 245102.
- Y. Shen, J. Zhou, T. Liu, Y. Tao, R. Jiang, M. Liu, G. Xiao, J. Zhu, Z.-K. Zhou, X. Wang, C. Jin and J. Wang, *Nat. Commun.*, 2013, **4**, 2381.
- H. Wang, D. W. Brandl, F. Le, P. Nordlander and N. J. Halas, *Nano Lett.*, 2006, **6**, 827–832.
- J. N. Anker, W. Paige Hall, O. Lyandres, N. C. Shah, J. Zhao and R. P. Van Duyne, *Nature Mater.*, 2008, **7**, 442–453.



Capped BNAs exhibit the unique ability to simultaneously enhance optical electric and magnetic fields by > 3 orders of magnitude.
234x146mm (96 x 96 DPI)